EXPERIMENTAL INVESTIGATIONS OF THE TURBULENT SWIRL FLOW IN STRAIGHT CONICAL DIFFUSERS WITH VARIOUS ANGLES

by

Dejan B. ILIĆ*, Miroslav H. BENIŠEK, and Đorđe S. ČANTRAK

Hydraulic Machinery and Energy Systems Department, Faculty of Mechanical Engineering, University of Belgrade, Belgrade, Serbia

Original scientific paper
DOI: 10.2298/TSCI????

Results of experimental investigations of the turbulent swirl flow in three straight conical diffusers with various diffuser total angles are presented in this paper. All three diffusers have the inlet diameter 0.4 m and total divergence angles 8.6°, 10.5° and 12.6°. The incompressible swirl flow field is generated by the axial fan impeller, and for each diffuser several regimes were achieved by changing rotation number. Original classical probes were used for measurements. The distributions of the average main swirl flow characteristics along the diffuser are shown. Distributions of the inlet Boussinesq number, outlet Coriolis coefficient, ratio of the swirl and completely axial flow loss coefficients at conical diffuser on the inlet swirl flow parameter are also presented.

Key words: *diffuser, turbulent swirl flow, loss coefficient.*

Introduction

Turbulent swirl flow is a complex phenomenon. It is a three-dimensional and anisotropic flow, with intensive diffusion processes, high dissipation rate, etc. This fluid flow has regions characterized by high vorticity. They often occur in technical practice and in nature as well.

Turbulent swirl flow occurs at the exit of the turbomachines, such as in the case of the flow at the diffuser inlet following the axial pump and fan impellers, or in the draft tubes following bulb turbines. These problems attract researches with the idea to increase energy efficiency, i.e. to achieve better power parameters (characteristics) of hydraulic turbomachines and systems.

An overview of the turbulent flow experimental research in diffusers is presented in papers [1],[2]. In the past two decades, research of the swirl flow in a conical diffuser is mainly performed by CFD, which is also upgraded with flow simulations in the turbine flow passages. It is also desirable, for good diffuser swirl flow prediction, to know the value of the Coriolis coefficient at the diffuser exit, because it has higher values than in the case for pure axial flow.

The main aim of this paper is to provide the integral characteristics of the turbulent swirl flow in straight diffusers with circular cross-section which are used with bulb turbines in

* Corresponding author; e-mail: dilic@mas.bg.ac.rs

hydropower plants. Study of the energy losses, which directly influence the hydraulic machinery efficiency, has focus on: determination of the ratio of swirl and pure axial flow loss coefficient in the straight conical diffusers, determination of the swirl flow coefficients in the cross-sections and the law of their behaving along the diffuser, calculation of the Coriolis coefficient and Boussinesq number for the swirl flow in cross-sections along diffuser and their dependence on the swirl flow parameters.

Paper [2] presents part of the experimental results for diffuser II with the angle 10.5°. New experimental results for all three angles, including the old one – diffuser II, are revealed here. Two new steel diffusers are designed and built, with a total divergence expansion angles: 8.6° - diffuser I and 12.6° - diffuser III.

Fluid flow separation for axial flow in diffusor could be presumed on the basis of the diffuser geometry (angle and area ratio). Namely, in the case of the non-swirl flow, for diffusers which are studied in this paper, assumption is that for total angles 8.6° and 10.5° separation doesn't exist, while with angle 12.6° separation should occur. Swirl flow relocates separation point downstream comparing to the non-swirl flow. The swirl flow gives more energy to the boundary flow, using the centrifugal force, so that the separation point can be avoid. Separation doesn't exist for swirl flows in diffusers even with angle 16°, if moderate circumferential flow is exerted at the diffuser inlet. It means that swirl flow in diffusers with angle 12.6° will not result with fluid flow separation.

Experimental test rig and methodology

Experimental test rig is shown in fig. 1. The same test rig was used for the turbulent swirl flow researches in all three conical diffusers. This test rig's primary use was for the axial fans experimental characteristics determination after the international standard ISO 5801. It was designed and constructed by Prof. Dr.-Ing. Zoran D. Protić† (1922-2010).

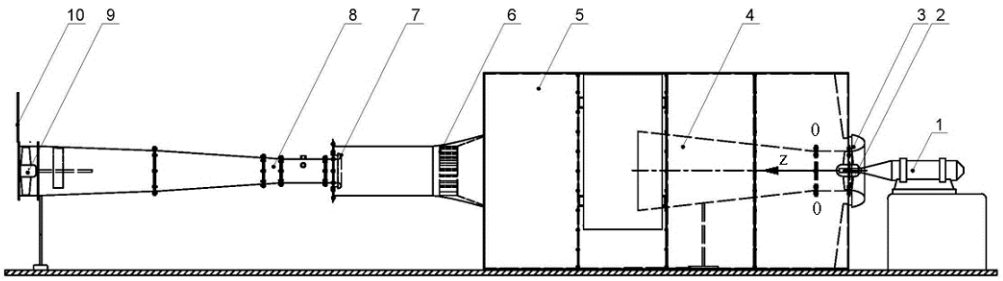

Figure 1. Test rig for experimental investigation

The incompressible swirl flow field is induced (fig. 1) by the axial fan impeller (2) with rotational speed controlled motor (1). The main geometry characteristics of the axial fan impeller, model AP 400, Minel, Serbia, are given in [3]. The axial fan is in-built in the straight pipe section with a profiled inlet nozzle (3). The impeller is followed by the straight conical diffuser (4), which is placed in the chamber (5). The test bed is equipped with the honey-comb (6), flow meter (7), pipe (8), booster fan (9) and flow regulator (10).

The main dimensions of the conical diffuser I, II and III are given in tab. 1. The diffusers have the same inlet diameter D_0 = 0.4 m and length L = 1.8 m. Velocity and pressure fields were measured at cross-sections given in tab. 2 and fig. 2, with 39 measuring points

along the diameter. The measurements are performed with unique home-made combined Prandtl and angular probes [4]-[5].

Investigations of the swirl flow performed with Conrad probe [6] and LDA systems, in diffusers [7], showed that the radial velocity is much smaller than circumferential and axial velocity $c_r << c_z$, $c_r << c_u$ for the used axial fan impeller. Furthermore, the assumption of two-dimensional flow was introduced on the basis of this. Also, the following values were measured: α, Δp_t ($\Delta p_t = p_t - p_a$), Δp ($\Delta p = p - p_a$), c ($c = (2(\Delta p_t - \Delta p)/\rho)^{1/2}$), c_z ($c_z = c \cdot \cos\alpha$) and c_u ($c_u = c \cdot \sin\alpha$).

Table 1. Dimensions of the conical diffuser

Diffuser	D_0 [m]	D_9 [m]	n_9 [-]	L [m]	α_{dif} [°]
I	0.4	0.67	2.81	1.8	8.6
II	0.4	0.73	3.33	1.8	10.5
III	0.4	0.80	4.00	1.8	12.6

Table 2. Positions of the measuring sections

Measuring sections (i)	z [m]	$z^* = z/L$ [-]
0	0	0
0*	0.065	0.036
1	0.2	0.11
2	0.4	0.22
3	0.6	0.33
4	0.8	0.44
5	1.0	0.56
6	1.2	0.67
7	1.4	0.78
8	1.6	0.89
9	1.8	1.00

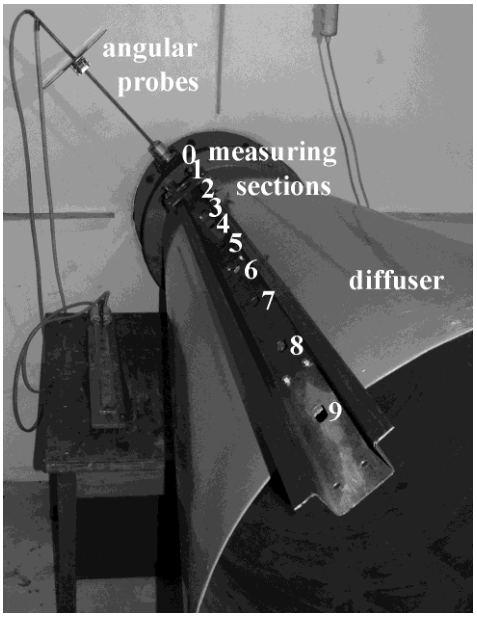

Figure 2. Positions of the measuring sections

Each measuring series, i.e. regime, is characterized by various parameters: Ω_0 - swirl flow parameter, Re - number and generated type of the swirl inflow profiles (velocity, pressure and circulation). The number of measuring series for diffuser I is seven (A-G, tab. 3) and for diffuser III it is five (A-E, tab. 3).

Table 3. Measuring series for diffuser

Diffuser I (8.6°)			Diffuser III (12.6°)			Diffuser II (10.5°)		
Series	Ω_0	$Re \cdot 10^{-5}$	Series	Ω_0	$Re \cdot 10^{-5}$	Series	Ω_0	$Re \cdot 10^{-5}$
A	0.74	2.59	A	0.13	0.52	X	2.79	2.66
B	0.95	1.46	B	0.52	1.30	Y	0.83	1.81
C	0.12	0.53	C	1.41	1.85	Z	3.55	2.70
D	1.29	1.85	D	3.22	2.07			
E	2.73	2.07	E	0.29	0.83			
F	3.58	2.17						
G	0.49	1.26						

For diffuser II measurements were performed for 22 measuring series (A-V), which is presented in [2], while three new series are added (X, Y and Z, tab. 3). These three new series are added to complete the results of investigation on diffuser II. Velocity and pressure fields in diffuser II at ten cross-sections (from 0 to 9, except 0*) were measured for all series. Velocity and pressure fields were measured in diffusers I and III at certain cross-sections.

The same definitions of the swirl flow characteristics [2] are used for all three diffusers. These relations for swirl flow characteristics in the cross-sections (i = 0, 0*, 1, 2 … 9) of the conical diffuser are presented herein.

Flow discharge is calculated as follows:

$$Q_i = 2\pi \int_0^{R_i} r c_z \mathrm{d}r \,,\ \dot{m}_i = \rho Q_i \,. \tag{1}$$

Mean circulation is given as below:

$$\overline{\Gamma}_i = \frac{4\pi^2}{Q_i} \int_0^{R_i} r^2 c_u c_z \mathrm{d}r \,, \tag{2}$$

while specific energy of the rotational flow is:

$$e_{c_{u_i}} = \frac{1}{\dot{m}_i} \int_{A_i} \frac{c_u^2}{2} \mathrm{d}\dot{m} = \frac{1}{R_i^2 c_{\mathrm{zm}_i}} \int_0^{R_i} c_u^2 c_z r \mathrm{d}r \,. \tag{3}$$

Specific energy of the axial flow is calculated in the following manner:

$$e_{c_{z_i}} = \frac{1}{\dot{m}_i} \int_{A_i} \frac{c_z^2}{2} \mathrm{d}\dot{m} = \frac{1}{R_i^2 c_{\mathrm{zm}_i}} \int_0^{R_i} c_z^3 r \mathrm{d}r \,, \tag{4}$$

while mean axial velocity is defined as follows:

$$c_{zm_i} = Q_i / (\pi R_i^2) \,. \tag{5}$$

Moment of the momentum for circumferential flow:

$$\dot{M}_{c_{u_i}} = \int_{A_i} r c_u \mathrm{d}\dot{m} = 2\pi\rho \int_0^{R_i} c_u c_z r^2 \mathrm{d}r = \frac{\dot{m}_i \overline{\Gamma}_i}{2\pi} \,, \tag{6}$$

while the moment of the axial flow is:

$$\dot{K}_{c_{z_i}} = \int_{A_i} c_z \mathrm{d}\dot{m} = 2\pi\rho \int_0^{R_i} c_z^2 r \mathrm{d}r = \beta_i \dot{K}_{c_{zm_i}} \,. \tag{7}$$

Moment of the mean axial velocity is:

$$\dot{K}_{c_{zm_i}} = \pi\rho c_{zm_i}^2 R_i^2 \,, \tag{8}$$

while the Boussinesq number [8] is defined as follows:

$$\beta_i = \dot{K}_{c_{z_i}} / \dot{K}_{c_{zm_i}} \,. \tag{9}$$

Swirl flow intensity is defined in the following way:

$$\theta_i = \frac{e_{c_{u_i}}}{e_{c_{z_i}}} = \frac{\int_0^{R_i} r c_u^2 c_z \mathrm{d}r}{\int_0^{R_i} r c_z^3 \mathrm{d}r} \,. \tag{10}$$

Instead of above shown swirl flow parameters, another several swirl flow parameters are defined by various authors [2]. These are: swirl flow parameter [9], swirl intensity [10], swirl number [11] and swirl intensity [12]. The relations between them are obvious and are presented in tab. 4.

Table 4. Swirl non-dimensional parameters

Swirl non-dimens parameters	Formula	Relations
Swirl flow parameter	$\Omega_i = \dfrac{Q_i}{R_i \overline{\Gamma}_i} = \dfrac{\left(\int_0^{R_i} rc_z \mathrm{d}r\right)^2}{R_i \int_0^{R_i} r^2 c_u c_z \mathrm{d}r}$	$\Omega_i \cdot S_i = \dfrac{1}{2\beta_i}$ for Rankin swirl flow: $\Omega_i \cdot S_i = \dfrac{1}{2}$
Swirl intensity	$\Omega_i^* = \dfrac{\dot{M}_{c_{u_i}}}{R_i c_{zm_i} \dot{m}_i} = \dfrac{2\int_0^{R_i} c_u c_z r^2 \mathrm{d}r}{R_i^3 c_{zm_i}^2}$	$\Omega_i^* = \dfrac{1}{2\Omega_i}$
Swirl number	$S_i = \dfrac{\dot{M}_{c_{u_i}}}{R_i \dot{K}_{c_{z_i}}} = \dfrac{\int_0^{R_i} c_z c_u r^2 \mathrm{d}r}{R_i \int_0^{R_i} c_z^2 r \mathrm{d}r} = \dfrac{2\int_0^{R_i} c_z c_u r^2 \mathrm{d}r}{\beta_i R_i^3 c_{zm_i}^2}$	$S_i = \dfrac{\Omega_i^*}{\beta_i} = \dfrac{2I}{\beta_i}$ for Rankin swirl flow: $S_i = \Omega_i^*$
Swirl intensity	$I = \dfrac{\dot{M}_{c_{u_i}}}{\dot{K}_{c_{zm_i}} D_i} = \dfrac{2\pi\rho\int_0^{R_i} c_u c_z r^2 \mathrm{d}r}{D_i \pi \rho c_{zm_i}^2 R_i^2} = \dfrac{\int_0^{R_i} c_u c_z r^2 \mathrm{d}r}{R_i^3 c_{zm_i}^2}$	$I = \dfrac{1}{4\Omega_i} = \dfrac{1}{2}\Omega_i^*$ for Rankin swirl flow: $I = \dfrac{\Omega_i^*}{2} = \dfrac{\Omega_i}{4}$

The swirl flow parameter Ω is more convenient, because it can be easily determined on the runner (impeller) outlet, i.e. at diffuser (draft tube) inlet if the flow discharge and the turbomachine specific flow energy are known only.

The swirl flow parameter [9] is defined as follows:

$$\Omega_i = \frac{Q_i}{R_i \overline{\Gamma}_i} = \frac{\left(\int_0^{R_i} rc_z \mathrm{d}r\right)^2}{R_i \int_0^{R_i} r^2 c_u c_z \mathrm{d}r}, \tag{11}$$

while Reynolds number:

$$\mathrm{Re}_i = \frac{c_{zm_i} 2R_i}{\nu}. \tag{12}$$

In the case of the swirl flow, considering the eq. (5) and (11) Reynolds number is correlated to the swirl flow parameter in the defined cross-section, with the kinematic viscosity and averaged circulation:

$$\mathrm{Re}_i = \frac{2}{\pi} \cdot \frac{\Omega_i \overline{\Gamma}_i}{\nu} . \tag{13}$$

Introducing that the air kinematic viscosity is constant, it is obtained for the diffuser inlet section that $\mathrm{Re}_0 = \mathrm{const} \cdot \Omega_0 \overline{\Gamma}_0$.

Specific swirl flow energy in each diffuser cross-section is:

$$\bar{e}_{\mathrm{S}_i} = \frac{2\pi}{\rho Q} \int_0^{R_i} r \Delta p_t c_z \mathrm{d}r . \tag{14}$$

Specific energy swirl flow losses along the straight conical diffuser from 0 to the *i*-th cross-sections are calculated as follows:

$$\Delta \bar{e}_{\mathrm{S}_i} = \bar{e}_{\mathrm{S}_0} - \bar{e}_{\mathrm{S}_i} . \tag{15}$$

The swirl flow energy loss coefficient is expressed as:

$$\zeta_{S_i} = \frac{2\Delta \bar{e}_{\mathrm{S}_i}}{c_{zm0}^2} . \tag{16}$$

The axial flow energy loss coefficient of the diffuser is introduced from [13]:

$$\zeta_{\mathrm{A}_i} = \mathrm{f}\left(\delta, \mathrm{Re}_0, \alpha_{\mathrm{dif}}, n_i\right), \tag{17}$$

where $\delta = \Delta / 2R_0$, $\mathrm{Re}_0 = c_{\mathrm{zm}0} 2R_0 / \nu$, and $n_i = A_i / A_0$.

The ratio of swirl and pure axial flow loss coefficient along the diffuser [2] is:

$$\frac{\zeta_{\mathrm{S}_i}}{\zeta_{\mathrm{A}_i}} = \mathrm{f}\left(\Omega_0\right), \tag{18}$$

where Ω_0 is the diffuser inlet swirl flow parameter $\Omega_0 = Q_0 / R_0 \overline{\Gamma}_0$.

The Coriolis coefficient at the diffuser outlet is then defined in the following way:

$$\alpha_{\mathrm{S}_9} = \frac{1}{R_9^2 \pi c_{zm9}^3} \int_9 c_9^2 c_{z9} \mathrm{d}A_9 = \frac{2}{R_9^2 c_{zm9}^3} \int_0^{R_9} r c_9^2 c_{z9} \mathrm{d}r . \tag{19}$$

Experimental results and discussion

Profiles of the total and static pressure become more uniform along the diffusers I, II and III. This is also shown for measurements in the diffuser II [2]. The total pressure has the lowest value in the vortex core region. Static pressure is the highest on the wall however it is the lowest in the vortex core region, where the value of relative static pressure can be negative. Axial velocity components have small values in the vortex core. In some cases, the reverse flow occurs. Circumferential velocity profile transforms downstream with the tendency to form a "solid body" profile on the diffuser outlet.

Swirl flow characteristic values for diffusers I, II (three added series) and III are calculated for each series in the measuring position $i = 0$ ($z = 0$) and presented in tab. 5. The Coriolis coefficient values and the ratio of swirl and pure axial flow loss coefficient at the diffuser outlet are also presented here.

It is noticeable that the specific swirl flow energy decreases exponentially, in the form $e_{\mathrm{si}} = e_{\mathrm{s}0} \cdot \exp(-\omega z^*)$, along the diffusers I and III (fig. 3) for all measuring series. Here, ω is the damping coefficient which depends on Ω_0, Re_0 and δ. This is also shown in the paper [2] for diffuser II.

Table 5. Characteristic diffuser swirl flow values

Diffuser I (8.6°)					
Ser.	Ω_0	α_{S9}	θ_0	β_0	ζ_{S9}/ζ_{A9}
A	0.74	3.41	0.74	1.12	11.10
B	0.95	2.26	0.35	1.16	7.89
C	0.12	34.63	3.43	2.83	240.31
D	1.29	1.57	0.20	1.14	4.96
E	2.73	1.19	0.04	1.14	3.25
F	3.58	1.20	0.03	1.12	3.47
G	0.49	3.50	1.26	1.18	22.51

Diffuser II (10.5°)					
Ser.	Ω_0	α_{S9}	θ_0	β_0	ζ_{S9}/ζ_{A9}
X	2.79	1.31	0.050	1.13	2.93
Y	0.83	3.38	0.500	1.15	6.35
Z	3.55	1.35	0.030	1.13	2.65

Diffuser III (12.6°)					
Ser.	Ω_0	α_{S9}	θ_0	β_0	ζ_{S9}/ζ_{A9}
A	0.13	46.37	1.99	3.54	121.82
B	0.52	4.15	1.15	1.16	11.93
C	1.41	1.94	0.16	1.15	3.44
D	3.22	1.70	0.03	1.15	2.41
E	0.29	11.48	1.82	1.55	31.04

Specific energy flow losses have increasing character along the diffusers I and III for all measuring series and depend on Ω_0, Re_0 and δ (fig. 4).

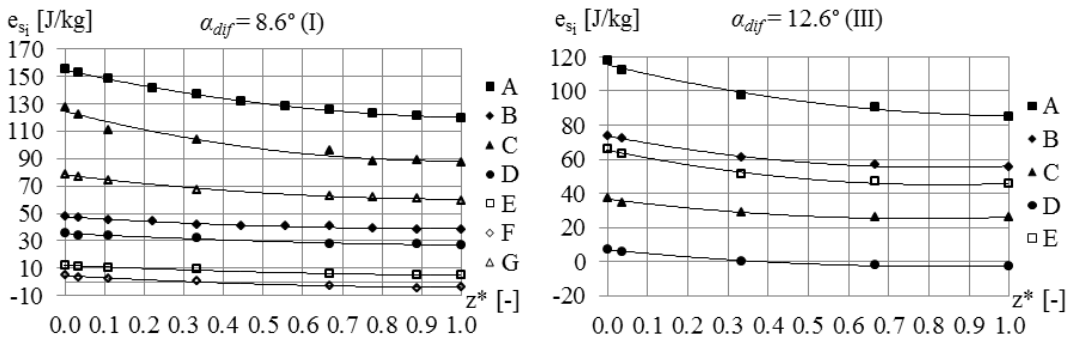

Figure 3. Swirl flow specific energy e_{si} along the diffuser ($z^* = z/L$): a) diffuser I for the measuring series: A to G, and b) diffuser III for the measuring series: A to E

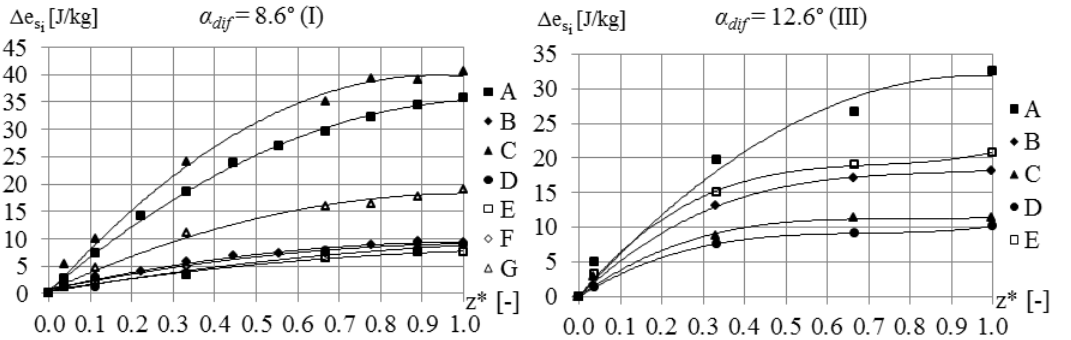

Figure 4. Swirl flow specific energy loss Δe_{si} along the diffuser ($z^* = z/L$): a) diffuser I for the measuring series: A to G, and b) diffuser III for the measuring series: A to E

Mean circulation distributions along the diffusers I and III (fig. 5) decrease linearly obeying the function $\Gamma_i = \Gamma_0 - \gamma z^* = \Gamma_0(1 - (\gamma/\Gamma_0)\cdot z^*) = \Gamma_0(1 - a\cdot z^*)$ for all measuring series. Here, Γ_0 is mean circulation for $z^* = 0$ and γ is the damping coefficient which depends on Ω_0, Re_0 and δ.

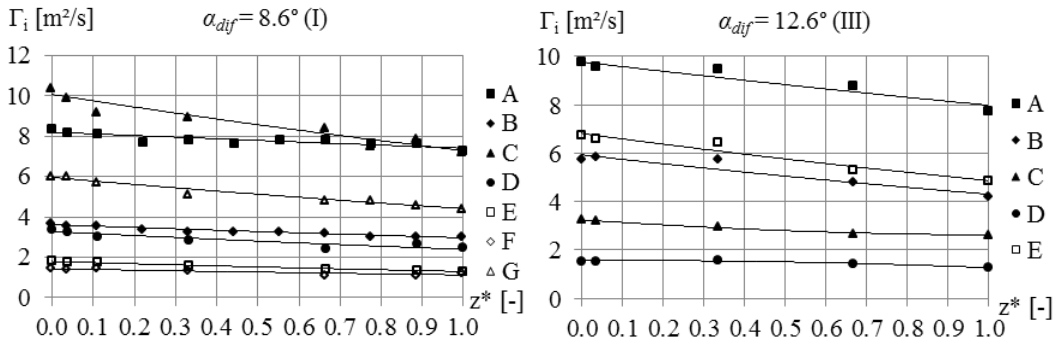

Figure 5. Mean circulation Γ_i along the diffuser ($z^* = z/L$): a) diffuser I for the measuring series: A to G, and b) diffuser III for the measuring series: A to E.

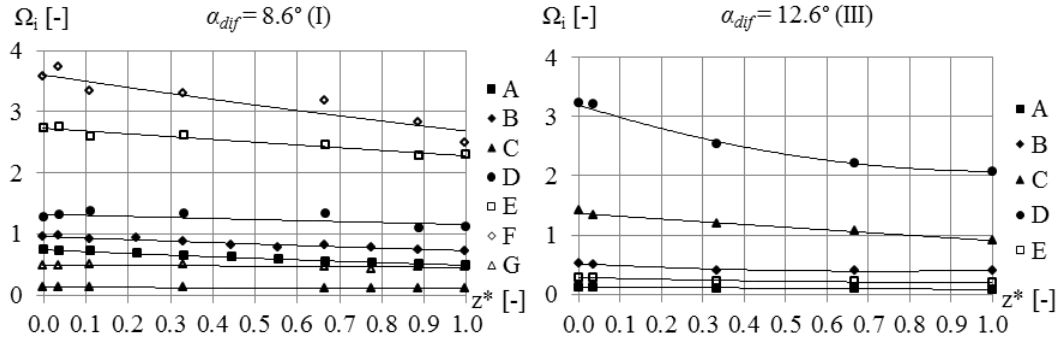

Figure 6. Swirl flow parameter Ω_i along the diffuser ($z^* = z/L$): a) diffuser I for the measuring series: A to G, and b) diffuser III for the measuring series: A to E

Swirl flow parameter transformation along the diffusers I and III (fig. 6) has the following character $\Omega_i = \Omega_0(1+c_1 z^* - c_2 z^{*2})^{-1}$ for all measuring series ($c_1 = L\mathrm{tg}\alpha_{\mathrm{dif}}/R_0 - a$, $c_2 = aL\mathrm{tg}\alpha_{\mathrm{dif}}/R_0 = ac_1 + a^2 = \mathrm{const}$ and $a = \gamma/\Gamma_0$).

Re-number influence on the distribution of the presented parameters is given through the influence of the swirl flow parameter and average circulation. Dependence of the Re_0-number of $\Omega_0\Gamma_0$ for all operating regimes of diffusers I and III, and some regimes of diffuser II is presented in the fig. 7.

Swirl flow characteristic values (β_0, ζ_{S9}/ζ_{A9} and α_{S9}) dependences on the swirl flow parameter Ω_0, for diffusers I, II and III, are presented in figs. 8, 9 and 10. These, the most important results, for three added and all other series, for diffuser II, are presented because they influence on the coefficient change reported in paper [2]. This is shown in tab. 6.

The Boussinesq number dependences on the swirl flow parameter Ω_0 for diffusers I and III (fig. 8) show that there is a great gradient in the region $\Omega_0 < 0.5$, but it slowly converges to $\beta = 1.02$ in the region $\Omega_0 \geq 0.5$. This is also shown for diffuser II [2].

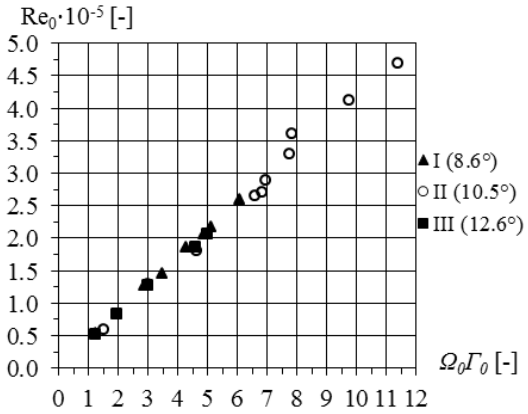

Figure 7. Reynolds number $\mathbf{Re_0}$ dependences of $\boldsymbol{\Omega_0\Gamma_0}$ for diffusers: I (measuring series: A to G), II (measuring series: A to I, X, Y, Z) and III (measuring series: A to E)

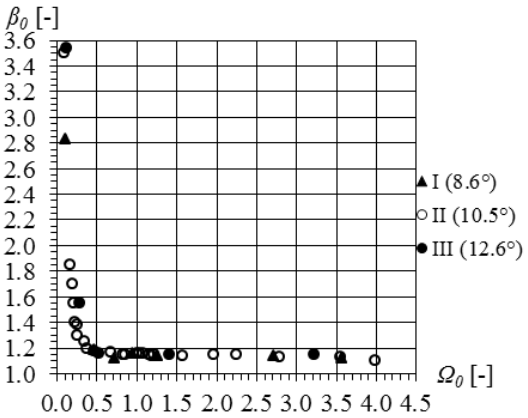

Figure 8. Boussinesq number $\boldsymbol{\beta_0}$ dependences on swirl flow parameter $\boldsymbol{\Omega_0}$ for diffusers: I (measuring series: A to G), II (measuring series: A to Z) and III (meas. series: A to E)

The Boussinesq number dependence on swirl flow parameter, at the entrance of the diffuser, for each diffuser (fig. 8), can be approximated by an exponential law:

$$\beta_0 = 1{,}1 + B/\Omega_0^p \,, \tag{20}$$

where the values of the coefficients B and p are provided in tab. 6.

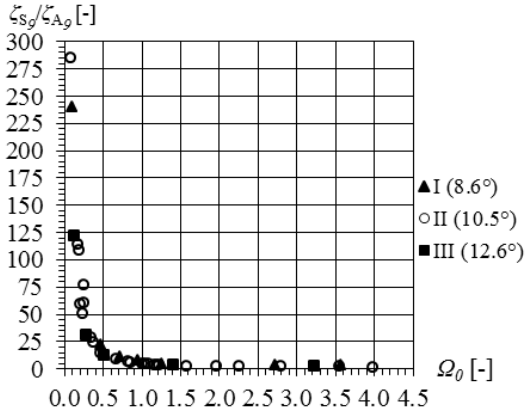

Figure 9. Ratio ζ_{S9}/ζ_{A9} dependences on swirl flow parameter Ω_0 for diffusers: I (measuring series: A to G), II ([2]) and III (measuring series: A to E)

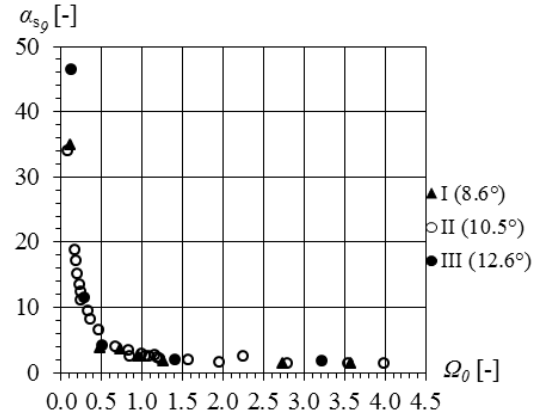

Figure 10. Outlet Coriolis coefficient α_{S9} dependences on swirl flow parameter Ω_0 for diffusers: I (meas. series: A to G), II (meas. series: A to Z) and III (meas. series: A to E)

The ratio of the swirl and pure axial flow loss coefficients ζ_{S9}/ζ_{A9} dependence on the inlet swirl flow parameter along the diffuser, for each diffuser (fig. 9), can be also approximated by the law:

$$\zeta_{S_9}/\zeta_{A_9} = 1 + k/\Omega_0^n , \tag{21}$$

where the values of the coefficients *k* and *n* are listed in tab. 6.

The outlet Coriolis coefficient dependence on the inlet swirl flow parameter, for each diffuser (fig. 10), can be approximated by an exponential law as follows:

$$\alpha_{S_9} = 1 + A/\Omega_0^m , \tag{22}$$

where the values of the coefficients A and m are given in tab. 6.

Table 6. Coefficients

Diffuser	I (α_{dif} = 8.6°)	II (α_{dif} = 10.5°)	III (α_{dif} = 12.6°)
B	0.0160	0.0191	0.0309
p	2.2143	2.0090	2.1082
A	0.9252	2.3713	1.1309
m	1.7013	1.1060	1.7809
k	6.17438	6.22244	3.77085
n	1.73197	1.59135	1.67243

Total specific energy loss Δe_{s9} of the turbulent swirl flow in the conical diffuser can be now calculated as follows:

$$\Delta\bar{e}_{S_9} = \zeta_{S_9} \cdot \frac{c_{zm_0}^2}{2} = \zeta_{A_9}\left(1 + \frac{k}{\Omega_0^n}\right) \cdot \frac{c_{zm_0}^2}{2} . \tag{23}$$

It is obvious that the outlet Coriolis coefficient has a great value when the swirl flow parameter Ω_0 is small (fig. 8). It means that the inlet mean circulation is strong and discharge is small. In the case of the great swirl parameter values Ω_0, when the circulation is weak and discharge is greater, the Coriolis coefficient decreases and tends to value α_A = 1.058.

The Coriolis coefficient for swirl flow at the diffuser outlet α_{S9} is very important for determination of the real swirl flow specific kinetic energy loss at the diffuser outlet. The value of the real specific kinetic energy loss Δe_{K9} is:

$$\Delta\bar{e}_{K_9} = \alpha_{S_9} \frac{\bar{c}_{zm_9}^2}{2} = \alpha_A\left(1 + \frac{A}{\Omega_0^m}\right)\frac{\bar{c}_{zm_9}^2}{2} , \tag{24}$$

where c_{zm9} is the mean velocity axial component $c_{zm9} = Q/A_9$.

Conclusions

This paper presents experimental investigations performed for three diffuser geometries α_{dif} = 8.6°, 10.5°, 12.6°. Part of the experimental results for diffuser II is shown in [2]. Geometry of the diffuser with α_{dif} = 10.5° is an adapted geometry of the draft tube of one bulb turbine.

It is demonstrated that it is very practical to use swirl number (Ω) for the case of the turbomachines as one of its characteristic parameters. A significant number of measurement series, characterized by the swirl flow parameters Ω_0, Re_0 numbers and various types of generated swirl inflow profiles are presented here.

The velocity and pressure experimental profiles transform intensively along the diffuser for all three diffuser angles.

The mean circulation decreases linearly downstream for all tested diffuser geometries.

It is shown that ratios of the loss coefficients for swirl and pure axial flow along the diffuser cross measuring sections depend only on the inlet swirl parameter Ω_0. This is more intense for lower values of the inlet swirl flow parameter Ω_0 and it is also the case for the Boussinesq number β_0 and outlet Coriolis coefficient α_{S9}. Obtained laws $\zeta_{S9}/\zeta_{A9} = f(\Omega_0)$ for all diffusers are given.

Dependences $\beta_0 = f(\Omega_0)$, $\alpha_{S9} = f(\Omega_0)$ and $\zeta_{S9}/\zeta_{A9} = f(\Omega_0)$ for all three diffuser angles have similar character, and it is not possible to derive their practical dependence. It could be concluded that diffuser I, with the smallest angle, has lower values β_0 and α_{S9}, for the same Ω_0, comparing to other two diffusers with wider angles.

The Coriolis coefficient, for the case of the turbulent swirl flow at the diffuser outlet, depends only on the inlet swirl flow parameter Ω_0. Value α_{S9} provides the possibility to determine the real swirl flow specific kinetic energy loss at the diffuser outlet. This conclusion is of great importance for the efficiency bulb turbine calculation.

Experimentally obtained velocity profiles for all series and diffusers have shown that there is no wall flow separation. The reason is the presence of the centrifugal forces which occur in the swirl flow.

Acknowledgment

This work was funded by the grant from the Ministry of Education, Science and Technological Development, Republic of Serbia (TR 35046), which is gratefully acknowledged.

Nomenclature

- c - local velocity, [ms^{-1}]
- c_r - radial velocity component, [ms^{-1}]
- c_u - circumferential velocity component, [ms^{-1}]
- c_z - axial velocity component, [ms^{-1}]
- L - diffuser length, [m]
- n_9 - area ratio (=A_9/A_0), [-]
- p_a - ambient pressure, [Pa]
- R - diffuser radius, [m]
- z - distance from diffuser inlet to specified diffuser cross section, [m]
- z^* - relative distance from diffuser inlet to specified diffuser cross section, [-]

Greek symbols

- α - flow angle, [°]
- α_{dif} - diffuser angle, [°]
- Δ - roughness, [m]
- Δp - relative static pressure, [Pa]
- Δp_t - relative total pressure, [Pa]
- δ - relative roughness, [-]
- N - kinematic viscosity, [m^{2}s^{-1}]
- ρ - fluid density, [kgm^{-3}]

References

[1] Azad, R.S., Turbulent Flow in a Conical Diffuser: A Review, *Experimental Thermal and Fluid Science, 13* (1996), pp. 318-337

[2] Benišek, M.H., *et al.*, Investigation of the Turbulent Swirl Flows in a Conical Diffuser, *Thermal Science, Vol. 14* (2010), Supplement 1, pp. S141 - S154

[3] Čantrak Đ., *et al.*, Investigation of the Turbulent Swirl Flow in Pipe Generated by Axial Fans using PIV and LDA Methods, *Theoretical and Applied Mechanics, Vol. 42* (2015), Issue 3, pp. 211-222

[4] Benišek, M., Investigation of the Swirl Flow in Long Lined Circular Pipes (in Serbian), Ph.D. thesis, Univ. Belgrade, Faculty of Mech. Eng., Belgrade, Serbia, 1979

[5] Benišek, M.H., *et al.*, Aplication of New Classical Probes in Swirl Fluid Flow Measurements, *Experimental Techniques, Vol. 34* (2010), Issue 3, pp. 74-81
[6] Benišek, M., *et al.*, Universal Calibration Characteristics Conrad Probe for Measures 3D Velocity, Pressure and Total Pressure of Stationary Inviscid Fluid Flow, *Proceedings of Metrological*, Yug. Cong., Novi Sad, Serbia, 2000
[7] Ilić, D.B., Swirl Flow in Conical Diffusers, Ph.D. thesis, Univ. Belgrade, Faculty of Mech. Eng., Belgrade, Serbia, 2013
[8] Čantrak, S., *Hydrodynamics – Selected Chapters* (in Serbian), Faculty of Mechanical Engineering, Belgrade, Serbia, 1998
[9] Strscheletzky, M., Equilibrium Forms of the Axisymmetric Flows with Constant Swirl in Straight, Cylindrical Rotation Geometries (in German), *Voith Forschung und Konstruktion*, *Heft 5* (1959), Aufsatz 1
[10] Kitoh, O., Experimental Study of Turbulent Swirl Flow in a Straight Pipe, *J. Fluid Mech., Vol. 225* (1991), pp. 445-479
[11] Mahmud, T., et al., Flow Characterizations of Swirl Coaxial Jets from Diverging Nozzels, *J. Fluid Eng., Vol. 109* (1987), pp. 275-281
[12] Baker, W., Sayre, C.L., Decay of Swirl Flow of Incompressible Fluids in Long Pipes, Flow: Its Meas. And Control in Sci. And Ind., *Proc. Symp.*, Pt. 1, Pittsburgh, USA, 1971, Vol l, pp. 301-312
[13] Povh, I.L., *Aerodynamic Experiments in Mechanical Engineering* (in Russian), Moscow, Leningrad, SSSR, 1974

Paper submitted: February 5, 2016
Paper revised: March 23, 2016
Paper accepted: April 29, 2016